

Chapter 4

Soil Acidification in German Forest Soils



**Henning Meesenburg, Winfried Riek, Bernd Ahrends,
Nadine Eickenscheidt, Erik Grüneberg, Jan Evers, Heike Fortmann,
Nils König, Amalie Lauer, Karl Josef Meiwes, Hans-Dieter Nagel,
Claus-Georg Schimming, and Nicole Wellbrock**

4.1 Introduction

The deposition of acidifying pollutants drastically altered the element cycles of forest ecosystems in large regions of the world (Ulrich et al. 1980; de Vries et al. 2014). Sulphur (S) was the major component of acid deposition since the beginning of industrialization until the 1980s, whereas the nitrogen (N) species nitrate (NO_3) and ammonium (NH_4) became more important since the 1990s (Schöpp et al. 2003). Besides its acidifying effect, deposition of N also causes an increasing nitrogen saturation of forest ecosystems (Aber et al. 1989, 1998) (see Chap. 5).

H. Meesenburg (✉) · B. Ahrends · J. Evers · H. Fortmann · N. König · K. J. Meiwes
Northwest German Forest Research Institute, Göttingen, Germany
e-mail: henning.meesenburg@nw-fva.de; bernd.ahrends@nw-fva.de; jan.evers@nw-fva.de;
heike.fortmann@nw-fva.de; nils.koenig@nw-fva.de; karl-josef.meiwes@nw-fva.de

W. Riek
Eberswalde Forestry State Center of Excellence, University for Sustainable Development,
Eberswalde, Germany
e-mail: winfried.riek@hnee.de

N. Eickenscheidt
State Agency for Nature, Environment and Consumer Protection of North Rhine-Westphalia,
Recklinghausen, Germany
e-mail: nadine.eickenscheidt@lanuv.nrw.de

E. Grüneberg · A. Lauer · N. Wellbrock
Thünen Institute of Forest Ecosystems, Eberswalde, Germany
e-mail: erik.grueneberg@thuenen.de; nicole.wellbrock@thuenen.de

H.-D. Nagel
Öko-Data, Ahrensfelde, Germany
e-mail: hans.dieter.nagel@oekodata.com

C.-G. Schimming
Christian-Albrechts University Kiel, Kiel, Germany
e-mail: cschimming@ecology.uni-kiel.de

If acids are introduced to soils, a reduction of acid neutralizing capacity (ANC) is caused. However, the decline of ANC isn't accompanied by an equivalent increase of free acidity, since many soil components contain neutralizing properties. Dependent on soil-forming substrate and acid-base status, several buffer ranges differing in buffer capacity and buffer rate become active over time under the influence of acid inputs (Table 4.1). A characteristic change of soil solution composition occurs at the transition between different buffer ranges (Ulrich 1987). If the aluminium (Al) buffer range is approached, the risk of toxic concentrations of Al ions in soil solution is significantly enhanced (Reuss and Johnson 1986). Elevated concentrations of free Al impede the nutrient uptake by tree roots and mycorrhiza (de Wit et al. 2010) and hamper the growth of microorganisms (Piña and Cervantes 1996). Under acid conditions solute Al forms stable complexes with phosphorus (P) and may thus reduce the P availability in soils (Hansen et al. 2007). Whereas in the soil solid phase the reduction of ANC due to acid inputs is common to all soils, adverse impacts of soil acidification such as pH decline and Al mobilization into soil solution are restricted to forest soils with low buffer capacity.

Acids are introduced to soils as strong mineral acids (sulphuric acid H_2SO_4 , nitric acid HNO_3) or generated through biochemical processes such as uptake of NH_4 and equivalent release of protons by tree roots or the nitrification of reduced N to HNO_3 . Since the anions NO_3^- and chloride (Cl^-) are only marginally adsorbed in soils, they are prone to leaching into deeper soil horizons or to the groundwater. To preserve electroneutrality anions have to be accompanied by an equivalent amount of cations (Seip 1980). The composition of these cations is controlled by the composition of exchangeable cations (Reuss and Johnson 1985). Acidification caused by strong mineral acids may thus affect deep soil horizons and also groundwater or surface waters. On the other hand, natural soil acidification by weak acids such as carbonic or organic acids, which are increasingly protonated if pH declines, is mostly limited to upper soil horizons. Under certain conditions, acidification due to deposition of H_2SO_4 can be delayed by the retention of sulphate (SO_4^{2-}) in the soil by adsorption to pedogenic hydroxides or by precipitation as Al hydroxy sulphate. The remobilization of previously stored SO_4^{2-} causes an equivalent release of acidity (Ulrich 1994).

Buffering of acids in forest soils in the long term is mainly provided by weathering of primary minerals (Ulrich 1983). In carbonate-free soils, the release of base cations (Ca, Mg, K, Na) from silicate minerals such as feldspars and clay minerals is the major proton consuming process (Fölster 1985; Tarrah et al. 2000). The release of structural Al during the weathering process usually results in the formation of interlayer Al hydroxides in clay minerals, which may reduce the cation exchange capacity drastically (Rich 1968). If acidification continues, proton buffering is also realized by the dissolution of these interlayer Al hydroxides, and cation exchange capacity may increase; however, previous values are usually not approached (Mareschal et al. 2013). For Germany, Ahrends et al. (2018) estimated an average base cation release due to weathering of $1.0 \text{ keq ha}^{-1} \text{ year}^{-1}$, $0.8 \text{ keq ha}^{-1} \text{ year}^{-1}$ of which are nutrient cations (Ca, Mg, K, see Chap. 2).

Table 4.1 Acid buffer ranges in aerated soils (Ulrich 1981, 1983) adjusted according to AK Standortskartierung (2003)

Buffer range	Carbonate (CaCO ₃)	Silicate	Exchange (exch.)	Aluminium (Al)	Al-Fe	Iron (Fe)
pH value	8.6–6.2	6.2–5.0	5.0–4.2	4.2–3.8	3.8–3.0	<3.0
Buffer rate	High	Low	Very high	High-medium	Medium in presence of soluble organic acids	
Major biogeochemical processes	Decalcification	Release of structural cations, regeneration of clay minerals	Leaching of exchangeable cations, decrease of exchange capacity	Resolution of Al silicates, destruction of clay minerals, protolysis of Al hydroxides	Fe mobilization as organic complexes	Bleaching under oxidative conditions

Consequences of soil acidification are the leaching of base cations (i.e. K, Mg, Ca) as counterions of mobile anions, the mobilization of protons, reactive Al and heavy metals and subsequent release into soil solution (Reuss and Johnson 1985). As base cations are important nutrients for forest trees, the loss of base cations may result in nutrient imbalances on base-poor sites (de Vries et al. 2014).

On the other hand, the uptake of nutrient cations may contribute to soil acidification, as an excess of ANC is removed from the soil (Ulrich 1994). The amount of ANC removal by biomass uptake depends on the preference of N uptake either as NH_4 or as NO_3 , resulting in an equivalent release of H^+ or OH^- via the root system, respectively (Reuss and Johnson 1986). For German NFSI plots on average, a net uptake of $0.5 \text{ keq ha}^{-1} \text{ year}^{-1}$ of nutrient cations was estimated, if stemwood utilization including bark is assumed (see Chap. 2). If NH_4 and NO_3 net uptake is balanced, this equals the net removal of ANC.

Soil acidification has been early claimed as a possible cause of forest decline, which was observed in central Europe since the late 1970s (Ulrich et al. 1980; Ulrich 1987). A consequence of this debate was the start of clean air policy, beginning with the Large Combustion Plant Directive in 1983 (13. BImSchV). This and other national and international measures (e.g. Convention of Long-range Transboundary Air Pollution CLRTAP; UNECE 1979) resulted in a significant reduction of deposition of acidity in Europe (Waldner et al. 2014).

Besides the CLRTAP, legal instruments for the prevention and compensation of acidification effects are the National Emissions Ceilings (NEC) Directive (2016/2284/EU), the German soil protection law (BBodSchG) and the European Water Framework Directive (WFD 2000/60/EC), which define criteria for the aspired state of soils and freshwater. Measures for the reduction of acid inputs are related to an ecological tolerable load. These critical loads provide “a quantitative estimate of an exposure to one or more pollutants below which significant harmful effects on specified sensitive elements of the environment do not occur according to present knowledge” (Spranger et al. 2015).

From the comparison with actual deposition loads, the compliance with or the exceedance of the critical loads can be derived. Further, the effectiveness of air pollution reduction measures can be controlled through the evaluation of deposition monitoring. The overarching environmental quality target for air pollution is the compliance with the critical loads for acidity (see Chap. 2). Moreover, the National Strategy on Biological Diversity in Germany aims to protect all sensitive ecosystems against acidification and eutrophication (BMU 2007).

Evidence for soil acidification caused by acid deposition proved by repeated soil sampling has been demonstrated in many studies (Falkengren-Grerup et al. 1987; Meesenburg et al. 2016; Blake et al. 1999; Johnson et al. 1994). So far, only few studies are showing recovery of forest soils from acidification (Lawrence et al. 2015), whereas recovery of surface waters due to declining deposition is a widespread phenomenon (Sucker et al. 2011; Wright et al. 2005; Stoddard et al. 1999).

The pH value, either measured in water ($\text{pH}(\text{H}_2\text{O})$) or in potassium chloride solution ($\text{pH}(\text{KCl})$), base saturation and the fractions of exchangeable acid cations (H^+ , Al, Mn, Fe) are used as indicators for the acid-base status of forest soils in this

study. The objective of this chapter is to evaluate if indications of recovery of forest soils from acidification in Germany are visible and to identify main drivers behind possible changes of soil acidity.

4.2 Acid-Base Status of German Forest Soils

4.2.1 Soil Acidity

For the characterization of soil acidity, the pH value in water ($\text{pH}(\text{H}_2\text{O})$) and in potassium chloride solution ($\text{pH}(\text{KCl})$) was determined. The $\text{pH}(\text{H}_2\text{O})$ indicates the effective soil acidity and shows distinct seasonal and episodic fluctuation. Through the introduction of potassium (K) during the $\text{pH}(\text{KCl})$ determination, the release of exchangeable aluminium (Al) and protons lowers the pH by 0.4–1.1 units. Thus the $\text{pH}(\text{KCl})$ is an indication of the potential soil acidity (Ulrich 1981).

The results of the second NFSI reveal a large spatial variability of pH in forest soils of Germany. On average, $\text{pH}(\text{H}_2\text{O})$ was 4.6 ± 0.02 , and $\text{pH}(\text{KCl})$ was 3.9 ± 0.02 in the organic layer. Limed plots showed higher pH values as compared to unlimed plots. The 10th percentile in the organic layer was 3.8 for $\text{pH}(\text{H}_2\text{O})$ and 2.9 for $\text{pH}(\text{KCl})$, and the 90th percentile was 5.8 for $\text{pH}(\text{H}_2\text{O})$ and 5.3 for $\text{pH}(\text{KCl})$. As compared to the organic layer, mean pH was slightly lower in the uppermost mineral soil layer and increased with depth. In 30–60 cm depth a mean $\text{pH}(\text{H}_2\text{O})$ of 5.2 ± 0.03 and $\text{pH}(\text{KCl})$ of 4.4 ± 0.03 was observed. The 10th percentile in this depth interval was 4.3 for $\text{pH}(\text{H}_2\text{O})$ and 3.6 for $\text{pH}(\text{KCl})$, and the 90th percentile was 7.5 for $\text{pH}(\text{H}_2\text{O})$ and 6.9 for $\text{pH}(\text{KCl})$.

The spatial distribution of pH values mainly reflects the different parent material of the soils (Fig. 4.1). High pH values were observed in soils developed from carbonatic bedrock, e.g. at the Swabian-Franconian Alb and in the Alps. Locally, also soils with intermediate basic-intermediate bedrock, e.g. tertiary basalts, show higher pH values in the topsoil (Meesenburg et al. 2009). Plots with acidic soils over the complete depth profile occur mainly in regions with soils developed from base-poor substrates, such as in the Black Forest, the Bavarian Forest, the Ore Mountains, the Harz Mountains and the North German lowlands with early Pleistocene sediments.

With respect to soil parent material groups, NFSI plots with soils from weathered carbonate bedrock revealed highest pH values, whereas lowest pH was observed for soils from base-poor unconsolidated sediments, soils from base-poor consolidated bedrock and loamy soils of the lowland (data not shown). Soils from basic-intermediate bedrock and soils from alluvial plains showed medium pH values, which were significantly different from base-poor and base-rich soil parent material groups in the organic layer.

The pH of the organic layer was lower under coniferous forest stand types than under deciduous and mixed stand types. This becomes more apparent, if unlimed plots for distinct soil parent material groups are compared. In the mineral soil, tree

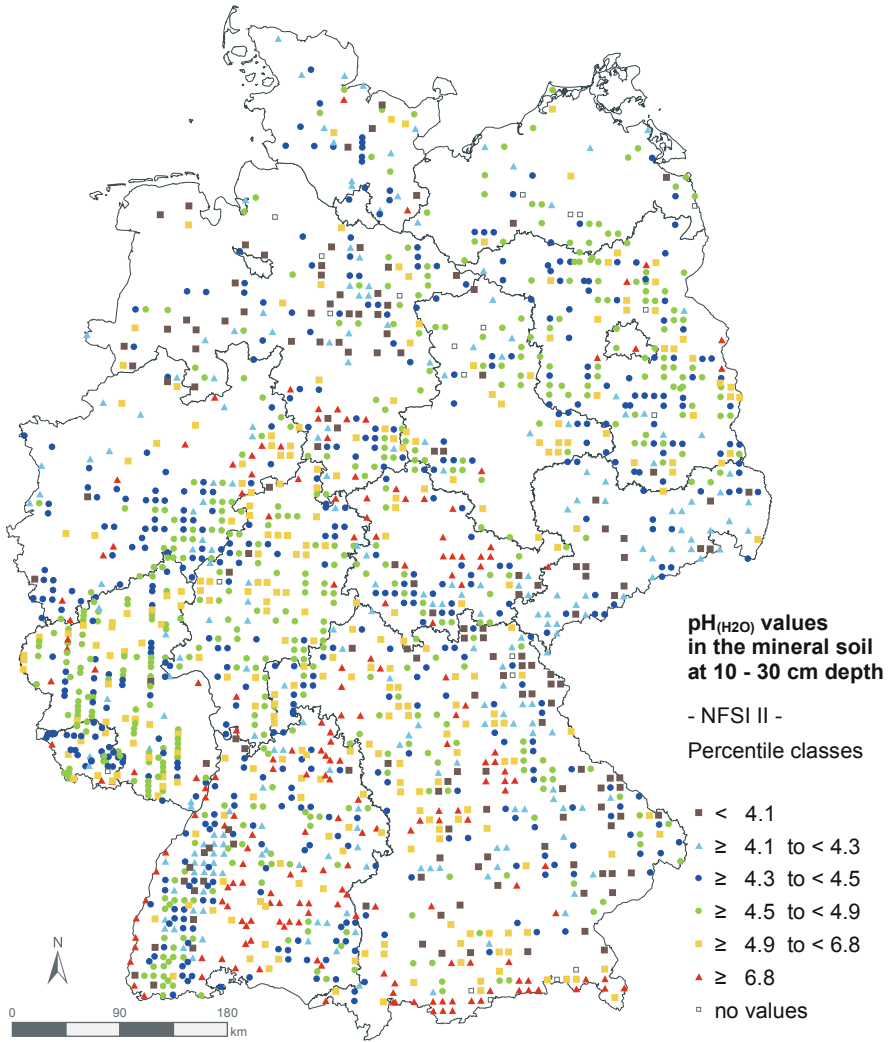


Fig. 4.1 pH(H₂O) values in the mineral soil at 10–30 cm depth of NFSI II

species-specific differences disappear with increasing depth. The observed pattern can be attributed to a higher base cation content of deciduous litter (Augusto et al. 2002; Jacobsen et al. 2002), but also to a preferential cultivation of coniferous tree species on acid organic layers.

The comparison between first and second NFSI reveal on average a significant increase of pH(H₂O) in the organic layer and in all depth intervals of the mineral soil (Fig. 4.2). The pH increase was highest in the organic layer ($0.013 \pm 0.0014 \text{ year}^{-1}$) and in the 0–5 cm interval of the mineral soil ($0.011 \pm 0.0011 \text{ year}^{-1}$). In the deeper mineral soil, the pH change was much smaller. For pH(KCl) a significant increase of

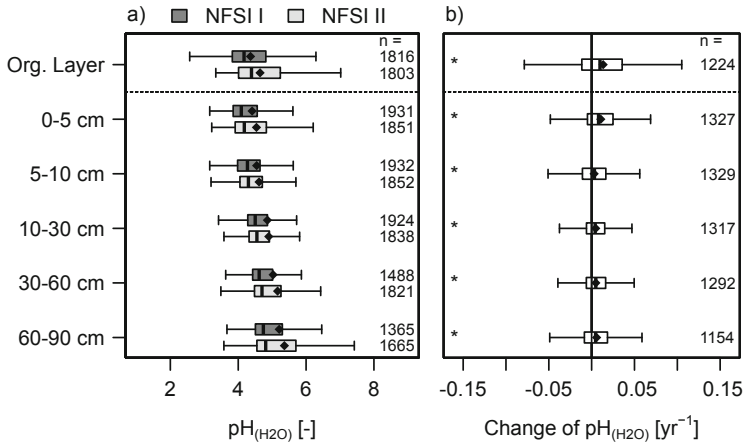


Fig. 4.2 $\text{pH}_{(\text{H}_2\text{O})}$ values in the organic layer and in the mineral soil layers for NFSI I and NFSI II (a, complete sample including bogs and organic soils) and differences of $\text{pH}_{(\text{H}_2\text{O})}$ values between NFSI I and NFSI II (b, paired sample without bogs and organic soils, *denotes significant change of $\text{pH}_{(\text{H}_2\text{O})}$, $p \leq 0.05$)

$0.004 \pm 0.0014 \text{ year}^{-1}$ pH units could only be observed for the organic layer, whereas the 5–10 cm interval showed a pH decrease of $0.004 \pm 0.001 \text{ year}^{-1}$ (not shown). The other sampling intervals revealed only insignificant changes. The pH increase in the topsoil is attributed primarily to the reduced deposition of acidity and to liming measures. The reduced leaching of basic cations from the organic layer may have contributed to the pH increase together with an increased contribution of base-rich litter from deciduous tree species, which were increasingly present at the plots since NFSI I.

The higher increase of $\text{pH}_{(\text{H}_2\text{O})}$ as compared to $\text{pH}_{(\text{KCl})}$ in all depth intervals may be attributed to a decrease of ionic strength of soil solution. For a given distribution of exchangeable cations, a decrease of ionic strength results in an increase of pH, which is more prominent for $\text{pH}_{(\text{H}_2\text{O})}$ than for $\text{pH}_{(\text{KCl})}$ as the latter is also determined by the exchanger composition (Reuss and Johnson 1986). A decrease of ionic strength of soil solution during the period from 1990 to 2006/2008 was demonstrated for several forested sites in northwest Germany (Klinck et al. 2012; Meesenburg et al. 2016).

According to the $\text{pH}_{(\text{H}_2\text{O})}$ value the samples can be attributed to pH buffer ranges (Ulrich 1983). Changes in the frequency of samples in the different buffer ranges between NFSI I and NFSI II illustrate changes in the acid-base status of the NFSI plots. As compared to NFSI I, an increase of samples within the exchange buffer range, silicate buffer range and the CaCO_3 buffer range of 9% in the 0–5 cm interval and of 5% in the 5–30 cm interval was observed leading to equivalent reductions in the Fe, the Fe-Al and the Al buffer range (Fig. 4.3). In the 60–90 cm interval, a 5% decrease occurred in the Al and exchange buffer range with a concurrent increase in the silicate and CaCO_3 buffer range. The shift between pH

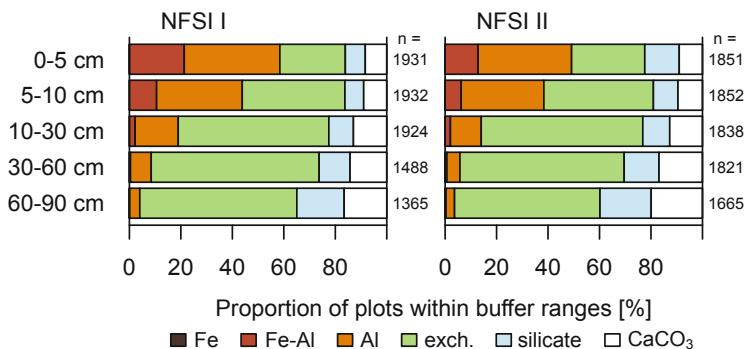
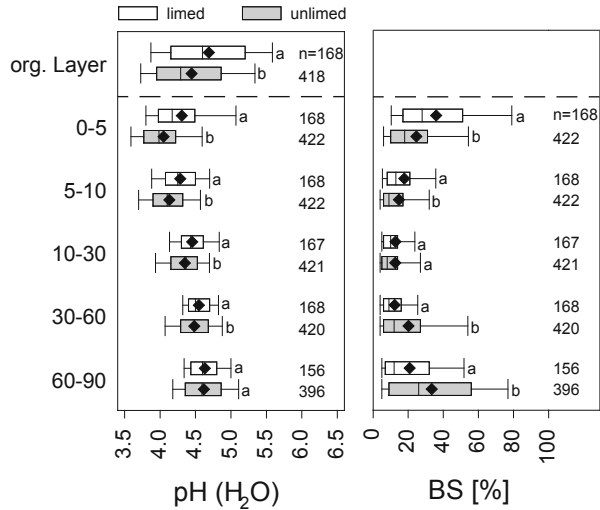


Fig. 4.3 Fractions of plots within different pH buffer ranges (according to Ulrich 1983) in the mineral soil for complete samples of NFSI I and NFSI II (Fe, Fe buffer range; Fe-Al, Fe-Al buffer range; Al, Al buffer range; exch., exchange buffer range; silicate, silicate buffer range; CaCO₃, carbonate buffer range)

buffer ranges was higher for limed as compared to unlimed plots. At unlimed plots, distinct changes of the frequency in the buffer ranges cannot be observed. This pattern is most probably a result of liming measures and a general decrease of the ionic strength of soil solution, which was observed for several intensive forest monitoring sites in northwestern Germany (Klinck et al. 2012). For the subsoil of unlimed NFSI plots, on average a balance between processes increasing and decreasing acidity can be assumed.

In the organic layer and in the mineral soil, up to 60 cm depth of acid-sensitive sites pH(H₂O) was significantly higher at limed as compared to unlimed plots (Fig. 4.4). Differences were less obvious for pH(KCl) (not shown). Between NFSI I and NFSI II, pH(H₂O) increased in the organic layer and in the mineral soil up to 10 cm depth both at limed and unlimed plots. Below 10 cm depth, unlimed plots showed no temporal change, whereas limed plots revealed an increase of pH(H₂O). For pH(KCl) no distinct pattern of changes was found. An exception from the observed pH increase in the organic layer is plots with pine as dominating tree species. For these plots pH(KCl) in the organic layer and up to 10 cm of the mineral soil decreased significantly. Pine stands are often cultivated on soil from base-poor unconsolidated sediments. Pine stands located in the northeastern German lowlands are mostly unlimed. In addition, many sites where high loads of basic dust were deposited in the last century are stocked with pine. These sites were acidified between NFSI I and NFSI II due to the leaching of bases (see Chap. 2).

Fig. 4.4 pH(H₂O) values (left) and base saturation (BS [%], right) for limed and unlimed acid-sensitive plots in the organic layer and mineral soil for NFSI II (acid-sensitive plots identified according to exchangeable aluminium pool in the subsoil)



4.2.2 Base Saturation

The acid-base status determines to a large degree the availability of nutrients in the soil, e.g. by the pH-dependent allocation of cations at the exchange sites. Thus, the nutrition of the forest stands is affected by soil acidification (see Chap. 9). The base saturation describes the proportion of effective cation exchange capacity in the soil occupied by Na, K, Mg and Ca. It serves as an indicator for the acid-base status of forest soils as the allocation of the exchange sites is strongly pH dependent. The introduction of acid cations can alter the base saturation significantly especially in the exchange buffer range. The occupation of exchange sites with acid cations such as Al, Mn, Fe and H⁺ is reciprocal to base saturation. Among the acid cations, Al usually constitutes the largest proportion.

Some exchange sites may also be occupied by NH₄ (Aber 1992). In the mineral soil, NH₄ can be retained at clay minerals (Davidson et al. 1991). As the ion radius of NH₄ is similar to that of K, in clay-rich soils NH₄ is fixed in the interlayers of 2:1 clay minerals and further not fully available for cation exchange (Nieder et al. 2011). However, as exchangeable cations were extracted with NH₄Cl solution (see Chap. 1), a quantification of the saturation of exchange sites with NH₄ is not possible for NFSI. In the mineral soil, soil solution concentrations of NH₄ are usually very low due to retention in the organic layer and nitrification (Brumme et al. 2009; Schwarz et al. 2016). Corre et al. (2007) found for German forest sites on a N deposition gradient, that microbial NH₄ retention was more important than abiotic NH₄ retention. Thus, it is assumed that exchangeable NH₄ only contributes to a small extent to total exchangeable cations.

Observations of base saturation from NFSI I and NFSI II are only available for the mineral soil. Hence, the medium-term availability of nutrient cations is characterized

for the organic layer by their aqua regia extractable stocks as these may be released when the organic layer is decomposed (see Chap. 3).

Mean base saturation in the uppermost 5 cm of the mineral soil was $41.5 \pm 0.8\%$ for NFSI II. It approached lowest values in 10–30 cm depth ($31.1 \pm 0.84\%$) and increased to deeper soil layers. In all soil layers a large span of base saturation from <4 to 100% was observed. Median values are consistently lower than arithmetic means for the different soil layers, e.g. 28% for the 0–5 cm depth and 12% for 10–30 cm.

Sites with high base saturation in the whole soil profile occur predominantly in regions with carbonate substrates, e.g. in the Alps and at the Swabian-Franconian Alb (Fig. 4.5). Low base saturation can be found in almost every region demonstrating the widespread loss of bases from forest soils in Germany. Forest soils with low base saturation over the whole profile were observed especially at low mountain ranges with base-poor silicate bedrock and at unconsolidated sandy substrates from Saalian sediments in the North German lowlands. Topsoils with low base saturation were observed in many substrates across Germany. Often forest soils with low base saturation occur in short distance to soils with high base saturation, which can be attributed to a high heterogeneity of site condition and to liming measures. Especially loamy soils of the lowlands and soils of alluvial plains showed a great variety of base saturation values and depth profiles (Fig. 4.6). Plots vegetated with deciduous tree species revealed significant higher base saturation in the upper 10 cm of the mineral soil as compared to coniferous tree species (Wellbrock et al. 2016). This pattern may be attributed to a higher base cation content of litter from deciduous tree species (Augusto et al. 2002; Jacobsen et al. 2002).

A significant increase of base saturation between NFSI I and NFSI II of $0.28 \pm 0.04\% \text{ a}^{-1}$ was observed in 0–5 cm depth of the mineral soil for the paired sample (Fig. 4.7). In contrast, a significant decrease of base saturation of $0.16 \pm 0.03\% \text{ a}^{-1}$, $0.3 \pm 0.04\% \text{ a}^{-1}$ and $0.28 \pm 0.04\% \text{ a}^{-1}$ in 10–30 cm, 30–60 cm and 60–90 cm, respectively, occurred. Accordingly, the fraction of plots within base saturation classes “very low” to “low to medium” (AK Standortskartierung 2003) decreased in the 0–5 cm depth from 65 to 52%, while plots within base saturation classes “medium” to “very high” increased (Fig. 4.8). The observed pattern of improved base saturation in the topsoil but ongoing soil acidification in the subsoil probably points to the effects of liming measures and reduced deposition of acidity, which are most prominent in the topsoil. Nitrification of reduced nitrogen and the remobilization of sulphur may delay the recovery of the subsoil. In addition, the uptake of base cations by the forest stands contributes to the loss of ANC from the subsoil.

Base saturation was higher on limed as compared to unlimed acid-sensitive plots of NFSI II down to 10 cm depth (Fig. 4.4). Acid-sensitive plots were identified according to the exchangeable Al pool in the subsoil. If the pool of exchangeable Al in 60–90 cm depth was higher than an equivalent of 3 to ha^{-1} of dolomitic lime, the respective NFSI plot was classified as acid sensitive (Höhle et al. 2018). For 45 long-term liming trials in northwest Germany, Guckland et al. (2012) found an 11% points increase of base saturation up to 40 cm depth. Unlimed plots of the NFSI II

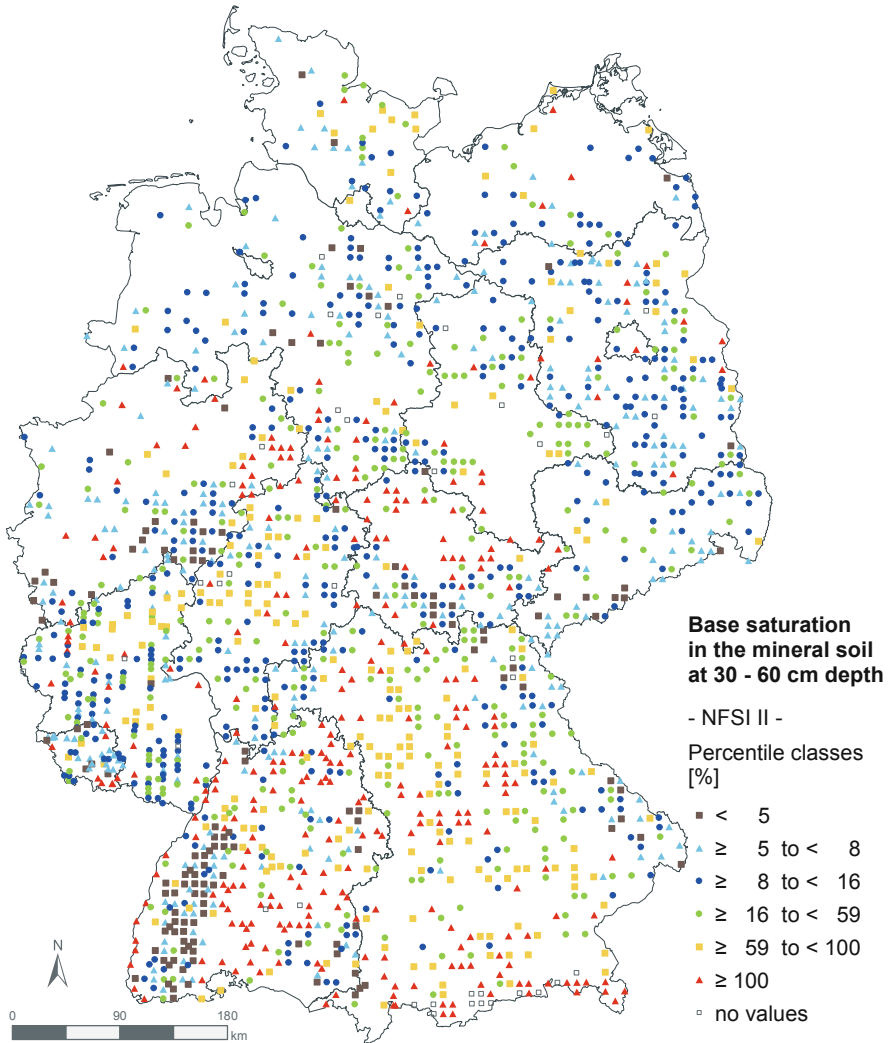
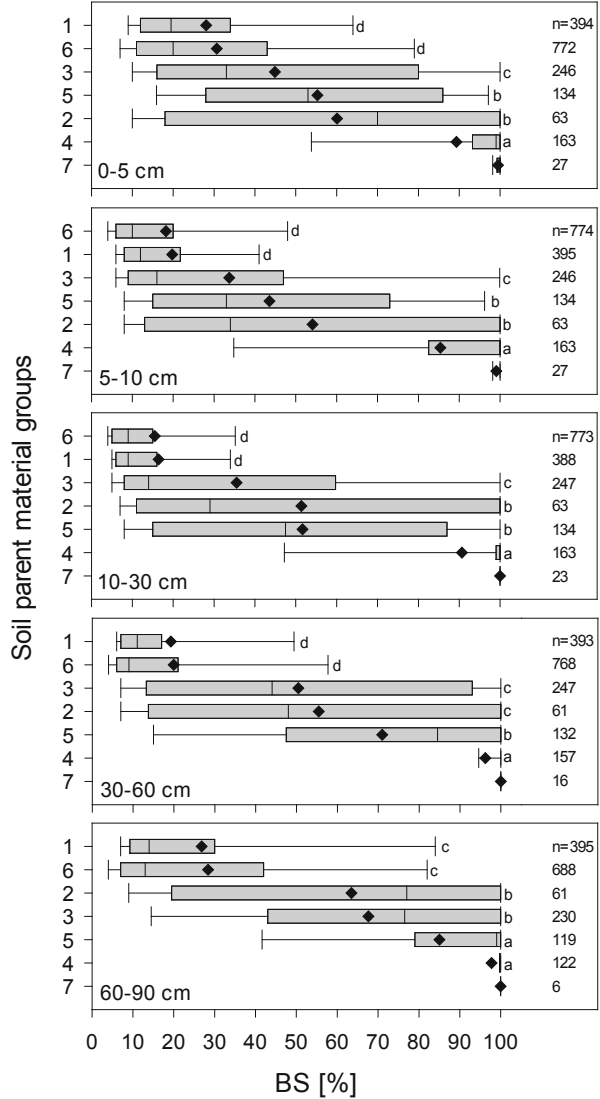


Fig. 4.5 Base saturation in % in the mineral soil at 30–60 cm depth of NFSI II

showed higher base saturation than limed plots in the subsoil (Fig. 4.4). This pattern may be interpreted with the selection of sites for liming, where most acidified sites are preferred. As the liming effect is mainly restricted to the topsoil, the sites selected for liming on average show lower base saturation. Between NFSI I and NFSI II, an increase of base saturation in the upper 30 cm of the limed plots and a decrease in 5–90 cm depth of the unlimed acid-sensitive plots were observed (Wellbrock et al. 2016).

An increase of base saturation between NFSI I and NFSI II occurred predominantly at loamy soils of the lowlands (0–5 cm depth), at soils from base-poor

Fig. 4.6 Base saturation for different soil parent material groups in the mineral soil for NFSI II (1, soils from base-poor unconsolidated sediments; 2, soils of alluvial plains; 3, loamy soils of the lowlands; 4, soils from weathered carbonate bedrock; 5, soils from basic-intermediate bedrock; 6, soils from base-poor consolidated bedrock; 7, soils from the Alps)



consolidated bedrock (0–10 cm depth) and at soils from weathered carbonate bedrock (0–10 cm depth, Fig. 4.9). A significant decrease of base saturation was observed at all depths for soils from base-poor unconsolidated sediments, in 10–90 cm depth at soils of alluvial plains, at loamy soils of the lowlands and at soils from base-poor consolidated bedrock in 30–60 cm depth and at soils from basic-intermediate bedrock in 10–30 cm depth (Fig. 4.9). The decrease of base saturation only took place at unlimed plots of all substrates, whereas liming gave rise to base saturation at soils from base-poor unconsolidated sediments (0–10 cm depth), at soils from basic-intermediate bedrock (0–5 cm depth) and at soils from

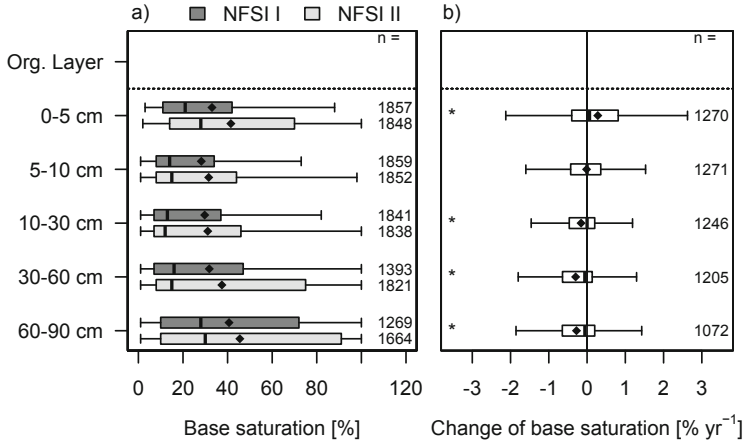


Fig. 4.7 Base saturation in the organic layer and in the mineral soil layers for NFSI I and NFSI II (a, complete sample including bogs and organic soils) and differences of base saturation between NFSI I and NFSI II (b, paired sample without bogs and organic soils)

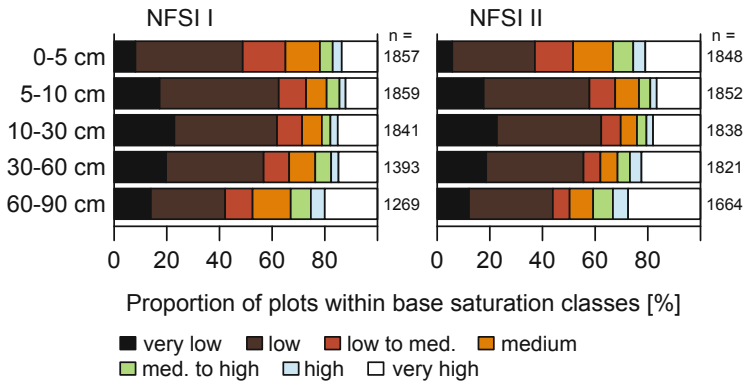


Fig. 4.8 Fractions of plots within different base saturation classes in the mineral soil for complete samples of NFSI I and NFSI II (base saturation classes according to AK Standortskartierung (2003); very low <7%, low 7–20%, medium to low 20–30%, medium 30–50%, medium to high 50–70%, high 70–85%, very high >85%)

base-poor consolidated bedrock (0–30 cm depth). Hence, liming seems to override effects of different substrates.

The effect of liming and other environmental and soil variables on the change of base saturation was analysed with a generalized additive model (GAM) (Hastie and Tibshirani 1990). A mass-weighted mean base saturation for the depth interval 0–90 cm of NFSI I and NFSI II was derived according to Spranger et al. (2015). The change of base saturation (BS) between NFSI I and NFSI II ($\Delta BS = BS_{NFSI II} - BS_{NFSI I}$) was analysed with various potential predictor variables (Table 4.2).

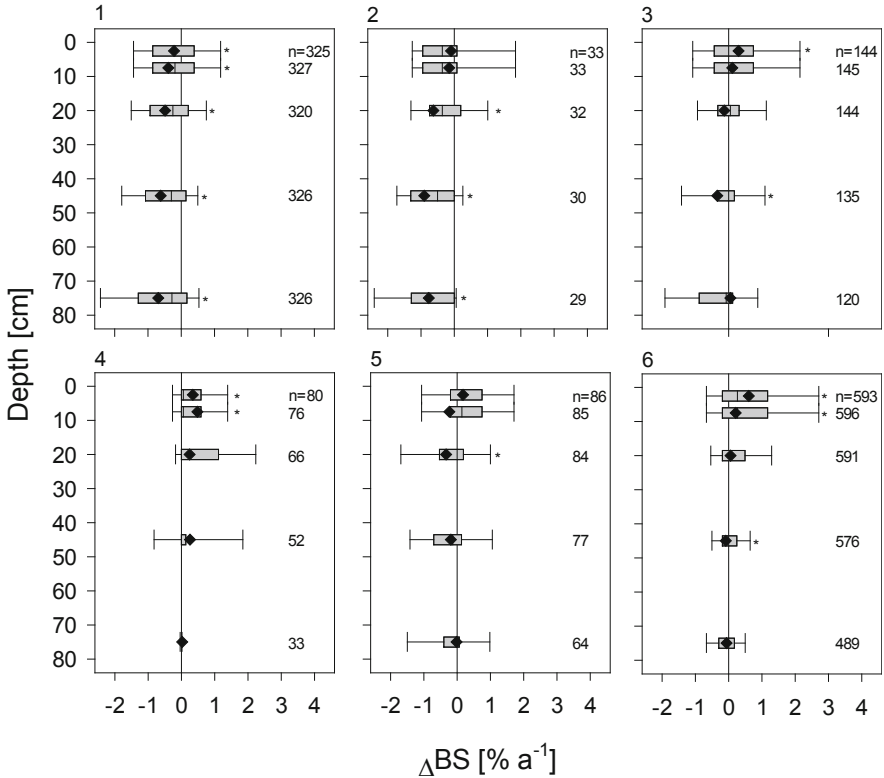


Fig. 4.9 Change of base saturation (ΔBS [% a^{-1}]) between NFSI I and NFSI II in the mineral soil for selected soil parent material groups (1, soils from base-poor unconsolidated sediments; 2, soils of alluvial plains; 3, loamy soils of the lowlands; 4, soils from weathered carbonate bedrock; 5, soils from basic-intermediate bedrock; 6, soils from base-poor consolidated bedrock)

For the development of the GAM, the general methodology of Wood (2006) was followed using the R-library *mgcv* (1.8–17). ΔBS and ΔCEC values outside the triple interquartile range ($3 \cdot \text{IQR}$) were excluded from the analysis. Furthermore one outlier detected from the residual plots of the final model was also excluded. For model building and variable preselection, the R add-on package *mboost* (2.8-1) was used (Hofner et al. 2011). To detect the optimal *mstop* values for application of the *mboost* function, a tenfold cross-validation was applied. Continuous variables were integrated as penalized splines in the model, each specific for limed and unlimed plots, respectively. Predictor variables significant at $p \leq 0.05$ were included in the model. The Ca stock in the organic layer and the mineral soil (0–90 cm), base saturation at NFSI I, the carbon stock in the organic layer, the carbon stock in the mineral soil (0–90 cm) and the K weathering rate (0–90 cm) were included in the final model (see Eq. 4.1, Table 4.3). Except the K weathering rate, each variable exhibits significantly different partial effects for limed and unlimed plots (Fig. 4.10a–e). The selected predictors account for 67% of the total variance:

Table 4.2 Predictor variables used in the generalized additive model (GAM) for the prediction of change of base saturation (0–90 cm) between NFSI I and NFSI II (Δ BS)

Predictor	Unit
S deposition	keq ha ⁻¹ a ⁻¹
N deposition	keq ha ⁻¹ a ⁻¹
BC deposition	keq ha ⁻¹ a ⁻¹
ACpotnet deposition	keq ha ⁻¹ a ⁻¹
Net biomass BC uptake	keq ha ⁻¹ a ⁻¹
Calcium weathering rate	keq ha ⁻¹ a ⁻¹
Magnesium weathering rate	keq ha ⁻¹ a ⁻¹
Potassium weathering rate	keq ha ⁻¹ a ⁻¹
BC release by silicate weathering	keq ha ⁻¹ a ⁻¹
Cation exchange capacity	mmol _c kg ⁻¹
Base saturation mineral soil 0–90 cm	%
Carbon stock organic layer	t ha ⁻¹
Carbon stock mineral soil 0–90 cm	t ha ⁻¹
Carbon stock organic layer + mineral soil 0–90 cm	t ha ⁻¹
Nitrogen stock organic layer + mineral soil 0–90 cm	t ha ⁻¹
C/N ratio	–
Calcium stock organic layer + mineral soil 0–90 cm	kg ha ⁻¹
Magnesium stock organic layer + mineral soil 0–90 cm	kg ha ⁻¹
Potassium stock organic layer + mineral soil 0–90 cm	kg ha ⁻¹
BC stock organic layer + mineral soil 0–90 cm	keq ha ⁻¹
Liming	Yes/no
Carbonates in soil	Yes/no
Stand type	Categorical
Soil type	Categorical
Soil class	Categorical
Soil parent material group	Categorical
Seepage flux	mm
Soil water content	m ³ m ⁻³
Mean air temperature	°C
Mean annual precipitation	mm
Stand type	Categorical
Federal state	Categorical
Latitude	GK4
Longitude	GK4

Table 4.3 Estimated coefficients and statistical characteristics of the model

	Est.	SE	edf
Parametric coefficients			
Intercept	-0.3173	0.2511	
LI = YES	1.7872*	0.6924	
Approximate significance of smooth terms			
$f_{LI,NO}(\log Ca)$			4.428***
$f_{LI,YES}(\log Ca)$			2.712***
$f_{LI,NO}(BS)$			4.044***
$f_{LI,YES}(BS)$			1.000***
$f_{LI,NO}(CO)$			2.997***
$f_{LI,YES}(CO)$			1.000***
$f_{LI,NO}(CM)$			1.000***
$f_{LI,YES}(CM)$			2.458***
$f_3(KW)$			2.352***

Est estimated parameter value, *SE* standard error, *edf* effective degrees of freedom, *Ca* calcium stock, *BS* base saturation, *CO* carbon stock in organic layer, *CM* carbon stock in mineral soil, *KW* K weathering rate, *LI* limed, Signif. codes: <0.001***, <0.05*

$$\begin{aligned}
\Delta BS_i = & \beta_0 + I_{\{LI=NO\}} f_{LI,NO}(\log Ca_i) + I_{\{LI=YES\}} f_{LI,YES}(\log Ca_i) \\
& + I_{\{LI=NO\}} f_{LI,NO}(BS_i) + I_{\{LI=YES\}} f_{LI,YES}(BS_i) \\
& + I_{\{LI=NO\}} f_{LI,NO}(CO_i) + I_{\{LI=YES\}} f_{LI,YES}(CO_i) \\
& + I_{\{LI=NO\}} f_{LI,NO}(CM_i) + I_{\{LI=YES\}} f_{LI,YES}(CM_i) \\
& + f_1(KW) + I_{\{LI=YES\}} \beta_1 + \varepsilon_i
\end{aligned} \tag{4.1}$$

with

ΔBS_i = change in base saturation between NFSI I and NFSI II at NFSI plot i [%]

β_0 = intercept

I = indicator function, denoted by $I_{\{condition\}} = \{(1, \text{if } LI = YES)/(0, \text{else})\}$

$f_{LI,p}$, ($p = NO, YES$) = to describe liming specific one-dimensional penalized regression splines

β_1 = parameter vector corresponding to LIME (LI)

Ca = calcium stock in organic layer + mineral soil 0–90 [kg ha⁻¹]

BS = base saturation at NFSI I in mineral soil 0–90 [%]

CO = carbon stock in organic layer [t ha⁻¹]

CM = carbon stock in mineral soil 0–90 [t ha⁻¹]

KW = K weathering rate in mineral soil 0–90 [kg ha⁻¹ a⁻¹]

LI = lime classes (NO, unlimed; YES, limed)

f_1 = one-dimensional penalized regression splines

ε_i = random error term, $\varepsilon_i \sim N(0, \sigma_\varepsilon^2)$

The Ca stock displays a positive partial effect on ΔBS , which is stronger for unlimed as compared to limed plots (Fig. 4.10a). Contrariwise, for base saturation at NFSI I, a negative effect with higher base saturation values is apparent (Fig. 4.10b).

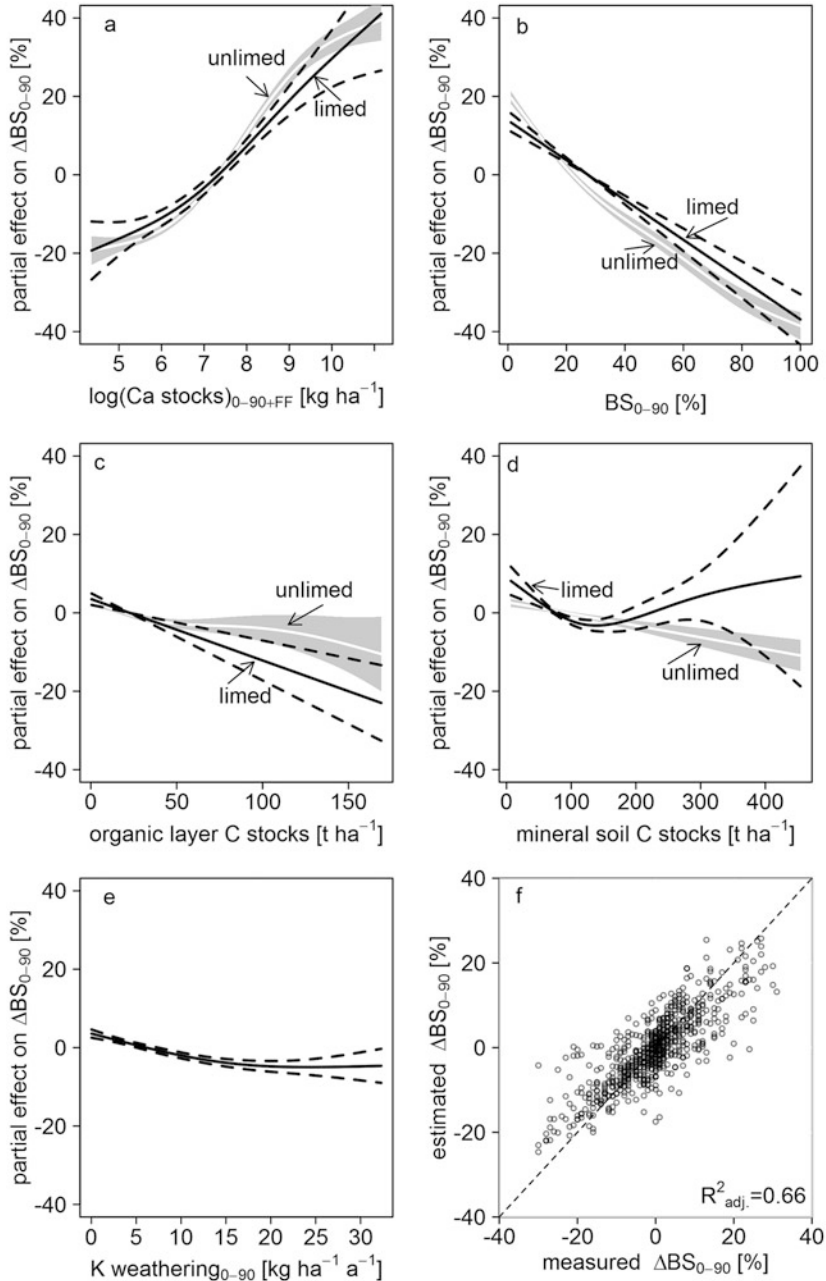


Fig. 4.10 Partial effects of Ca stock in organic layer + mineral soil 0–90 (a), base saturation 0–90 (b), carbon stocks in organic layer (c), carbon stocks in mineral soil (d), K weathering rates (e) and the relationship between measured and estimated base saturation changes in the soil 0–90 (ΔBS) (f). Dashed lines indicate 95% pointwise prognosis intervals

For the interpretation of these effects, a strong correlation between base saturation and calcium stock in soil ($r_{\text{spear}} = 0.7^{***}$) should be considered. The negative relation of base saturation with ΔBS may indicate that sites with very low base saturation had reached a low level, where the flux of base cations was restricted (Horn et al. 1989). Sites with higher base saturation have a higher potential for decrease of base saturation especially at sites where sulphate is released into soil solution. In addition, sites affected by deposition of fly ashes (see Chap. 3) show a high base saturation at NFSI I, hence a disproportional high reduction of base saturation (Riek et al. 2012). The effect size of organic layer and mineral soil carbon stock is lower than that of Ca stock and base saturation. On sites with a higher organic layer carbon stock, there is a higher retention of base cations in the organic layer and consequently a lower availability of base cations in the mineral soil (Fig. 4.10c). The model identified also an effect of mineral soil carbon stocks on ΔBS which is stronger on limed plots for very low carbon stocks (Fig. 4.10d). Although the effect of K weathering on ΔBS is only weak, it may be interpreted as a disproportional high decrease of base saturation on sandy sites with a high proportion of illite-like clay minerals, e.g. soils from base-poor unconsolidated sediments (Fig. 4.10e). From Fig. 4.10f no systematic deviation of the relation between estimated and observed change in base saturation is visible.

The sensitivity of ΔBS for limed and unlimed plots with respect to base saturation between 10 and 25% for different levels of Ca stock (600 and 900 kg ha⁻¹) and organic layer carbon stocks (20 and 40 t ha⁻¹) is visible in Fig. 4.11. The other variables included in the GAM were held constant at the median of NFSI II. Liming generally increases ΔBS especially where a large reduction of base saturation occurs indicating an efficient mitigation of further soil acidification after liming. With regard to a different depth interval (0–90 cm) considered in this study, the effect size is comparable to the findings of Guckland et al. (2012) for sites in northwest Germany, who found differences in base saturation of 20%, 5% and 3% for the depth intervals 0–10 cm, 10–20 cm and 20–40 cm of limed as compared to unlimed plots, respectively. A strong effect of organic layer carbon stocks on Ca and Mg retention and base saturation changes was also described by Guckland et al. (2012). In summary, model results suggest that ΔBS is mainly dependent on the soil pools of basic substances at NFSI I, which is modified with respect to liming and soil organic matter status.

4.2.3 *Aqua Regia Extractable Ca Stocks*

The mean stocks of aqua regia extractable Ca in the organic layer amounted to 288 ± 9 kg ha⁻¹ for the NFSI II. High amounts of Ca were found predominantly at sites with carbonate-containing bedrock and at limed plots (Fig. 4.12). Low Ca amounts were observed in soils from base-poor substrates at low mountain ranges and in the North German lowlands. Evers et al. (2016) found for the state of Hesse a decrease of Ca stocks in the organic layer and an increase in the mineral topsoil

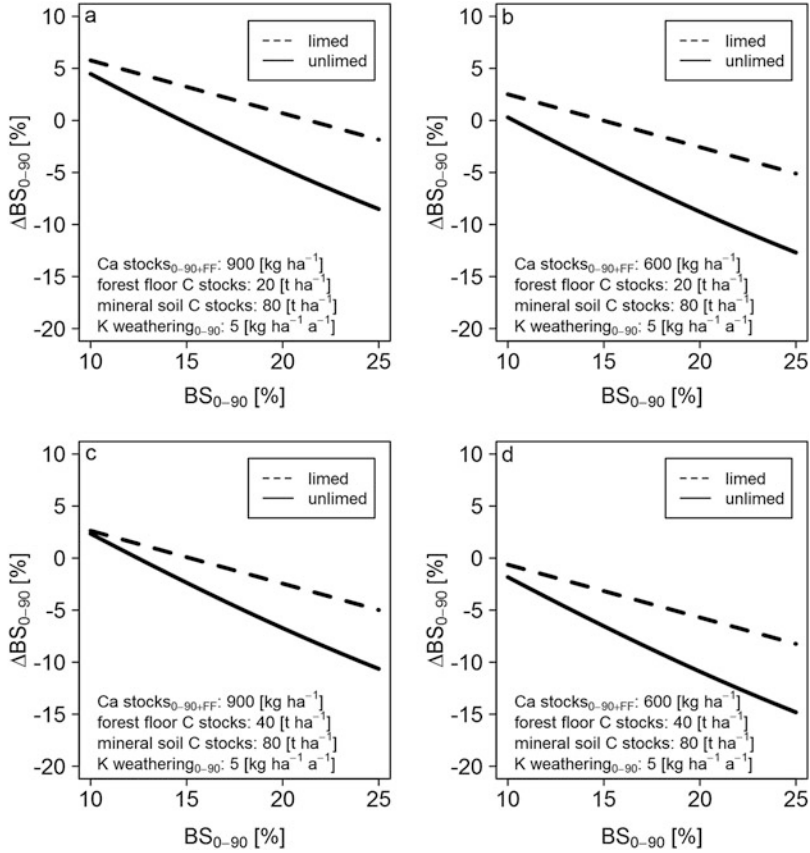


Fig. 4.11 Partial effects of base saturation on base saturation changes between NFSI I and NFSI II (Δ BS) for different levels of Ca stocks and organic layer carbon stocks. Other variables held constant

between NFSI I and NFSI II. The spatial and temporal pattern of Mg stocks was similar to Ca yet at a lower level (not shown).

4.2.4 Comparison with Long-term Studies on Soil Acidification

The time period between NFSI I and NFSI II is characterized by strong reductions of acid deposition. However, even stronger reductions occurred prior to NFSI I beginning in the 1980s. In order to compare changes in the acid-base status of forest soils between NFSI I and NFSI II to a longer time period, long-term studies from intensive

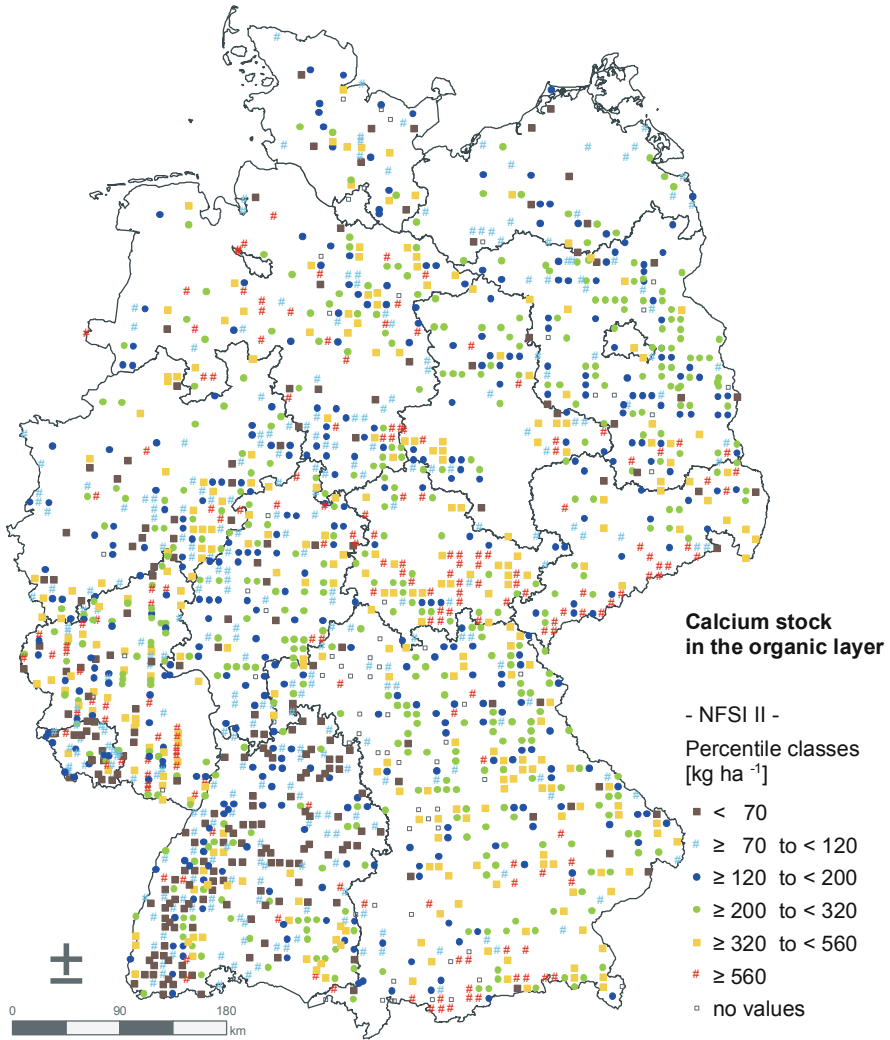


Fig. 4.12 Calcium stock in kg ha⁻¹ in the organic layer of NFSI II

monitoring plots from northwestern Germany were evaluated with respect to soil acidity.

At two intensive monitoring plots of the ICP Forests Level II programme at Solling, northwestern Germany, stocked with European beech (Level II plot 304) and Norway spruce (Level II plot 305) 11 and 12 inventories of the mineral soil, respectively, have been conducted between 1966 and 2010. At both plots, base saturation showed a decreasing trend between the late 1960s and the beginning of the 2000s, whereas a slight recovery was observed within this century (Figs. 4.13 and 4.14). Recovery was more distinctive in the upper soil layers, whereas the subsoil

Fig. 4.13 Long-term development of base saturation over depth at Level II plot 304 Solling beech

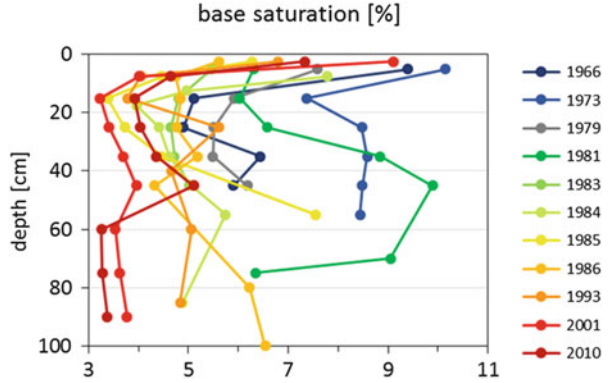
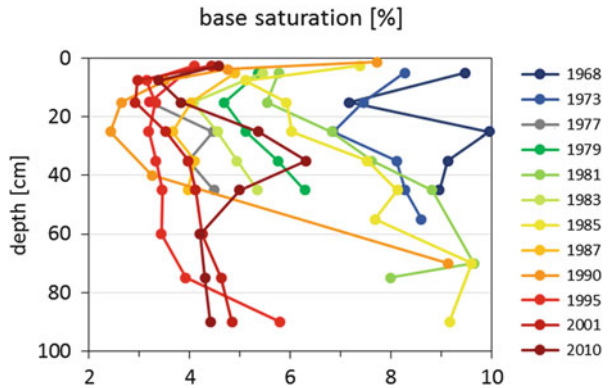


Fig. 4.14 Long-term development of base saturation over depth at Level II plot 305 Solling spruce



experienced a further acidification. The loss of base cations from the mineral soil until the 1990s was partly compensated by an accumulation in the organic layer (Meiwes et al. 2009). Since then, base cations were released into the mineral soil due to enhanced decomposition of the organic layer (Meesenburg et al. 2016).

At long-term monitoring plots at substrates with low buffer capacity and soil samplings before 1985, strong decreases of base saturation in the 0–30 cm layer of the mineral soil occurred before 1990 (Fig. 4.15). The decrease ceased at those plots approximately between 1995 and 2005, and a slight increase of base saturation can be assumed since then. The time period, when soil acidification was reversed at these plots, falls in between NFSI I and NFSI II, which might explain opposite trends of soil acidification found at the NFSI plots.

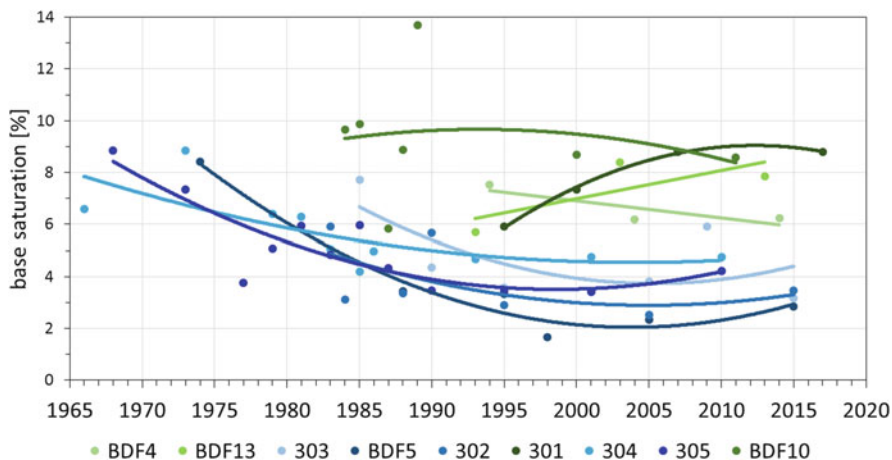


Fig. 4.15 Long-term development of base saturation at 0–30 cm depth of the mineral soil at intensive monitoring plots in northwest Germany. 301 to 305 refer to ICP Forests Level II plots, BDF4 to BDF13 to permanent soil monitoring plots; plots with soils from base-poor consolidated bedrock are in blue colour; plots with soils from base-poor unconsolidated sediments are in green colour; trend lines are second-order polynomial functions, except for plots with only three samplings, where a linear trend was applied

4.2.5 Case Study on Soil Acidification in the State of Brandenburg

A special pollution situation in the northeastern German lowlands became evident in the NFSI of the federal state of Brandenburg (Riek et al. 2015). An important outcome of this survey was that acidification of many forest soils in Brandenburg and neighbouring areas proceeded at an above-average rate in the period between NFSI I (1992) and NFSI II (2007). A decrease in the pH(KCl) values was recorded in the organic layer and the mineral topsoil to 30 cm depth, whereas pH(KCl) changes were insignificant in the subsoil. The base saturation as a sensitive indicator of soil acidification decreased significantly in all depths of the examined soil body (0–140 cm depth), and the Ca and Mg stocks have changed from predominantly low-medium to low (Ca) and from low to very low (Mg), respectively (valuation levels by AK Standortskartierung 2016).

The leaching of Ca and Mg ions, which had previously been deposited by flying ash from brown coal power plants, is regarded as a major cause for this obviously strong decrease of pH and base saturation in a relatively short period. A pronounced loss of base cations was recorded especially for those soils that had unusually high base saturations with respect to these usually nutrient-poor sandy soils at the time of NFSI I (Fig. 4.16).

Regionally occurring high pH(KCl) values in the mineral topsoil of the NFSI II sample, with simultaneously low values in the subsoil, also provide a clear indication for a still persisting effect of the former atmospheric deposition of basic dust. In

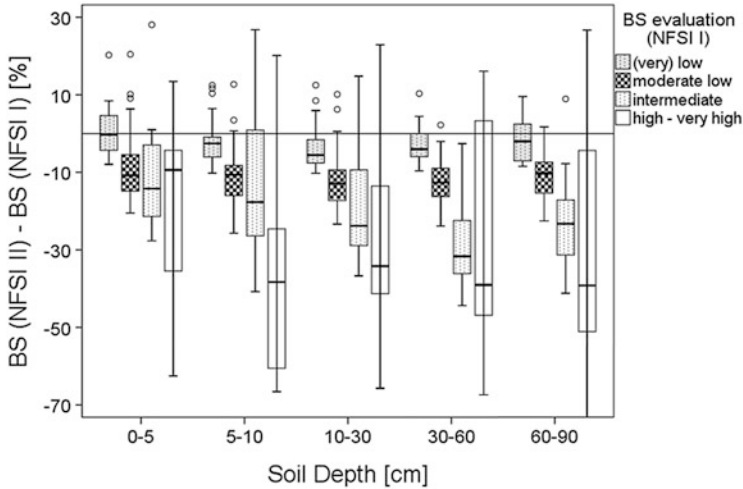


Fig. 4.16 Difference between base saturation (BS) from NFSI II and NFSI I in the state of Brandenburg, stratified by soil depth and evaluation level of base saturation at the time of NFSI I (evaluation levels according to AK Standortskartierung 2003), without hydromorphic and carbonate-containing soils ($n = 126$)

addition, local maxima of the base cation stocks are currently still found in the former dust deposition areas in southern Brandenburg. Noteworthy are the natural nutrient-poor inventory plots of this old moraine area, which still have very high Ca and Mg fractions of the cation exchange capacity despite a general reduction of base saturation between NFSI I and NFSI II. The depth profiles of base saturation at NFSI plots affected by fly ashes do not fit well to any of the depth profile types of base saturation defined in Chap. 2.

The former GDR brown coal production amounted to 85.2 million tons and peaked at 312.2 million tons in the mid-1980s (Buck 1996). The use of lignite in power plants grew steadily until the year 1989. It was increasingly burned as raw brown coal in the industrial agglomeration areas of the GDR. According to studies in the Bitterfeld area by Koch et al. (2001), the fly ashes consisted of high proportions of Ca and Mg oxides. The dusts were partly deposited in the vicinity of emission sources and due to emission with high chimneys also transported over long distances settling particularly at forest ecosystems because of their high surface roughness.

On the basis of deposition measurements since the 1960s (Möller and Lux 1992), coal mining statistics (Statistik der Kohlenwirtschaft e.V. 2015) and extensive analyses of bark samples on the grid of the forest condition survey of the former GDR in the years 1985 and 1988 (Stöcker and Gluch 1992; Kallweit et al. 1985), both the temporal and the spatial distribution of the base cation deposition were roughly calculated (Riek et al. 2015). According to these estimations approximately $50 \text{ kg ha}^{-1} \text{ year}^{-1}$ of Ca was deposited on average into pine stands in the state of Brandenburg at the time of the highest incidence of atmospheric pollution in the 1980s. A mean cumulative Ca deposition in the order of 2.2 t ha^{-1} for the period

from 1945 to 1990 is estimated according to this approach. This corresponds to an amount of lime of 6 t ha^{-1} (CaCO_3 content: 90%) over a period of 45 years, with which a large part of the acid sulphur deposition could be buffered. After cessation of emission of these specific atmospheric pollutants during the early 1990s, the accumulated mobile anions of sulphuric acid were leached, taking corresponding amounts of Ca and Mg ions with them.

Thus, it is assumed that the reduced base saturation recorded in the NFSI II represents a more natural state than the artificially elevated values at the time of the NFSI I in the regions previously affected by dust deposition.

4.3 Conclusions

The results of NFSI II demonstrate first achievements of environmental policy and forest management for the recovery of forest soils from acidification. The widespread acidification of topsoils and depletion of bases, which was observed during NFSI I, has been reduced. The recovery from acidification was highest in the organic layer and decreased with depth of the mineral soil. However, $\text{pH}(\text{KCl})$ decreased further especially at sites in the northeastern German lowlands. Where forest sites were limed, a significant increase of $\text{pH}(\text{KCl})$ until 10 cm depth was observed. The pH increase can be attributed to decreased deposition of acidity and to liming measures. A larger increase of $\text{pH}(\text{H}_2\text{O})$ as compared to $\text{pH}(\text{KCl})$ is due to the decrease of the ionic strength of soil solution after deposition reduction.

According to the main buffer mechanisms the sampled soil intervals can be assigned to buffer ranges. Due to changes of soil pH, the distribution of NFSI plots among the buffer ranges changed as well. The rise of pH in the topsoil resulted in an increase of plots within the exchange to CaCO_3 buffer range, whereas plots within the Fe to Al buffer range decreased. In the 60–90 cm depth interval the proportion of plots in the Al and exchange buffer range decreased in favour of the silicate and CaCO_3 buffer range. The shift in the distribution of plots among buffer ranges was mainly caused by liming.

Base saturation increased in the topsoil between NFSI I and NFSI II, which was significant for the paired sample in the 0–5 cm interval. However, a significant decrease of base saturation was observed below 10 cm depth. Limed plots showed a significant increase of base saturation in the upper 30 cm of the mineral soil, and base saturation in this depth range was higher as compared to unlimed plots.

The Al saturation of the NFSI plots showed a depth gradient, which was inverse to the depth gradient of base saturation. Aluminium saturation was on average $40.2 \pm 0.62\%$ in the 0–5 cm depth achieving a maximum of $62.3 \pm 0.79\%$ in 10–30 cm depth and decreasing values with increasing depth. Average Mn, Fe and H saturation was highest in the uppermost depth interval (0–5 cm) with values of $2.5 \pm 0.08\%$, $3.1 \pm 0.08\%$ and $12.8 \pm 0.31\%$, respectively, and decreased with increasing depth.

Mean stocks of aqua regia extractable Ca and Mg in organic layers of German forest soils were $288 \pm 8.5 \text{ kg ha}^{-1}$ and $73 \pm 2.7 \text{ kg ha}^{-1}$, respectively, for NFSI II. They were increasing with increasing depth achieving $1895 \pm 177 \text{ kg ha}^{-1}$ and $1403 \pm 62 \text{ kg ha}^{-1}$ of Ca and Mg, respectively, in 5–10 cm depth. The spatial distribution of nutrient cations was mainly related to the parent material of the soils with high stocks in soils from weathered carbonate bedrock and in soil from basic-intermediate bedrock, whereas low stocks were found in soils from base-poor substrates. Mean stocks of exchangeable nutrient cations (Ca, K, Mg) for the whole soil profile (0–90 cm) were $6670 \pm 274 \text{ kg ha}^{-1}$, $609 \pm 15.7 \text{ kg ha}^{-1}$ and $1206 \pm 62.3 \text{ kg ha}^{-1}$, respectively.

Liming between NFSI I and NFSI II exert a major effect on the acid-base status and the nutrient availability of forest soils. Limed sites reveal higher pH and base saturation as compared to unlimed sites. In addition, stocks of exchangeable Ca and Mg are significantly higher up to 30 cm depth.

At NFSI II plots, lower pH(KCl) values were observed in coniferous stands than in deciduous stands in the organic layer and in the mineral soil up to 10 cm depth. These differences were less distinctive in deeper soil layers.

Generally, the acid-base status of forest soils in Germany improved between NFSI I and NFSI II due to a strong reduction of acid deposition. The statistical evaluation showed a major impact of liming and the acid-base status at NFSI I on the base saturation change until NFSI II. In addition, carbon stocks in the organic layer and mineral soil exhibit a modifying influence. Soil acidification was decelerated or even reversed inducing a decreased Al concentration in soil solution with corresponding reduced toxic stress to tree roots and microorganisms. Especially those sites, which are limed and vegetated with deciduous tree species, showed indications of recovery. At limed sites the regeneration extended even to the subsoil. However, unlimed acid-sensitive sites revealed an ongoing acidification of the subsoil with corresponding losses of base cations. Major causes are the still substantial deposition of nitrogen species with subsequent generation of acidity through uptake and nitrification processes and the remobilization of previously retained sulphur. In addition, the loss of alkalinity through the uptake of nutrient cations gained increasing importance during the last decades because of increased growth rates and decreased importance of other sources of acidity. Owing to the nationwide reduction of acid inputs, the relative spatial variability of soil acidity increased. A regional peculiarity are the deposits of basic dust in parts of the northeastern German lowlands, which were subject to a strong leaching from the soils but still cause a higher level of alkalinity at some sites.

With respect to an aspired recovery of the acid-base status of forest soils in Germany, the following recommendations can be deduced from the results of NFSI:

- Further reduction of deposition of acidity to a level below critical loads of acidity
- Liming of acidified soils in order to accelerate the regeneration process and to compensate nutrient losses due to introduced mobile anions
- Limitation of nutrient removal with biomass extraction at nutrient-poor and acid-sensitive sites

- Promotion of deep-rooting tree species in order to enhance the zone, where mineral weathering contributes to the biogeochemical cycling of base cations

The above-mentioned adaptation options should be combined based on a site-specific evaluation of the current acid-base status and expected pathways of forest development.

References

- Aber JD (1992) Nitrogen cycling and nitrogen saturation in temperate forest ecosystems. *Trends Ecol Evol* 7:220–224
- Aber JD, Nadelhoffer KJ, Steudler P, Melillo JM (1989) Nitrogen saturation in northern forest ecosystems. *Bioscience* 39(6):378–386
- Aber JD, McDowell W, Nadelhoffer K, Magill A, Berntson G, Kamakea M, McNulty S, Currie W, Rustad L, Fernandez I (1998) Nitrogen saturation in temperate forest ecosystems – hypotheses revisited. *Bioscience* 48(11):921–934. <https://doi.org/10.2307/1313296>
- Ahrends B, Klinck U, Klinck C, Weis W (2018) Herleitung flächiger Verwitterungsraten. *Freiburger Forstl. Forschung* 101:113–149
- AK Standortkartierung (2003) Forstliche Standortaufnahme: Begriffe, Definitionen, Einteilungen, Kennzeichnungen, Erläuterungen, 6th edn. IHW-Verlag, Eiching near Munich
- AK Standortkartierung (2016) Forstliche Standortaufnahme: Begriffe, Definitionen, Einteilungen, Kennzeichnungen, Erläuterungen, 7th edn. IHW-Verlag, Eiching near Munich
- Augusto L, Ranger J, Binkley D, Rothe A (2002) Impact of several common tree species of European temperate forests on soil fertility. *Ann For Sci* 59(3):233–253. <https://doi.org/10.1051/forest:2002020>
- Blake L, Goulding K, Mott C, Johnston A (1999) Changes in soil chemistry accompanying acidification over more than 100 years under woodland and grass at Rothamsted Experimental Station, UK. *Eur J Soil Sci* 50(3):401–412
- BMU (2007) National strategy on biological diversity. BMU, Berlin
- Brumme R, Meesenburg H, Bredemeier M, Jacobsen C, Schönfelder E, Meiwes K, Eichhorn J (2009) Changes in soil solution chemistry, seepage losses, and input–output budgets at three beech forests in response to atmospheric depositions. In: Brumme R, Khanna P (eds) *Functioning and management of European beech ecosystems*. Ecological studies, vol 208. Springer, Berlin, pp 303–336
- Buck HF (1996) Umweltpolitik und Umweltbelastung. In: *Die wirtschaftliche und ökologische Situation der DDR in den 80er Jahren*. Springer, pp 223–266
- Corre MD, Brumme R, Veldkamp E, Beese FO (2007) Changes in nitrogen cycling and retention processes in soils under spruce forests along a nitrogen enrichment gradient in Germany. *Glob Chang Biol* 13(7):1509–1527
- Davidson E, Hart S, Shanks C, Firestone M (1991) Measuring gross nitrogen mineralization, and nitrification by ^{15}N isotopic pool dilution in intact soil cores. *J Soil Sci* 42(3):335–349
- de Vries W, Dobbertin MH, Solberg S, Van Dobben HF, Schaub M (2014) Impacts of acid deposition, ozone exposure and weather conditions on forest ecosystems in Europe: an overview. *Plant Soil* 380(1–2):1–45
- de Wit HA, Eldhuset TD, Mulder J (2010) Dissolved Al reduces mg uptake in Norway spruce forest: results from a long-term field manipulation experiment in Norway. *For Ecol Manag* 259(10):2072–2082. <https://doi.org/10.1016/j.foreco.2010.02.018>
- Evers J, Paar U, Schönfelder E (2016) Bodenchemische Kenngrößen in Hessen. In: Paar U, Evers J, Dammann I, König N, Eichhorn J (eds) *Waldbodenzustandsbericht für Hessen: Ergebnisse der*

- zweiten Bodenzustandserhebung im Wald (BZE II). Beitr Nordwestdeutsche Forstliche Versuchsanstalt, vol 15, pp 123–215
- Falkengren-Grerup U, Linnermark N, Tyler G (1987) Changes in acidity and cation pools of south Swedish soils between 1949 and 1985. *Chemosphere* 16(10–12):2239–2248
- Fölster H (1985) Proton consumption rates in Holocene and present-day weathering of acid forest soils. In: Drever JI (ed) *The chemistry of weathering*. Springer, Dordrecht, pp 197–209
- Guckland A, Ahrends B, Paar U, Dammann I, Evers J, Meiwes KJ, Schönfelder E, Ullrich T, Mindrup M, König N, Eichhorn J (2012) Predicting depth translocation of base cations after forest liming: results from long-term experiments. *Eur J For Res* 131(6):1869–1887. <https://doi.org/10.1007/s10342-012-0639-0>
- Hansen K, Vesterdal L, Bastrup-Birk A, Bille-Hansen J (2007) Are indicators for critical load exceedance related to forest condition? *Water Air Soil Pollut* 183(1–4):293–308
- Hastie T, Tibshirani R (1990) *Generalized additive models: monographs on statistics and applied probability*. Chapman and Hall, Boca Ratan, FL
- Hofner B, Müller J, Hothorn T (2011) Monotonicity-constrained species distribution models. *Ecology* 92(10):1895–1901
- Höhle J, Bielefeldt J, Dühnelt P-E, König N, Ziche D, Eickenscheidt N, Grüneberg E, Hilbrig L, Wellbrock N, Kompa T (2018) Bodenzustandserhebung im Wald – Dokumentation und Harmonisierung der Methoden. Thünen Working Paper. Johann Heinrich von Thünen Institute, Braunschweig. <https://doi.org/10.3220/WP1526989795000>
- Horn R, Schulze E-D, Hantschel R (1989) Nutrient balance and element cycling in healthy and declining Norway spruce stands. In: Schulze ED, Lange OL, Oren R (eds) *Forest decline and air pollution*. Springer, Berlin, pp 444–455
- Jacobsen C, Rademacher P, Meesenburg H, Meiwes K (2002) Gehalte chemischer Elemente in Baumkompartimenten – Literaturstudie und Datensammlung. *Berichte des Forschungszentrums Waldökosysteme*, vol 69. Göttingen, Germany, 80 pp
- Johnson A, Andersen S, Siccama T (1994) Acid rain and soils of the Adirondacks. I. Changes in pH and available calcium, 1930–1984. *Can J For Res* 24(1):39–45
- Kallweit R, Kaatzsch S, Strube M, Keller E (1985) Bioindikation über Kiefern und Fichtenborken. ZUG, Umweltlabor, Wittenberg
- Klinck U, Rademacher P, Scheler B, Wagner M, Fleck S, Ahrends B, Meesenburg H (2012) Ökosystembilanzen auf forstwirtschaftlich genutzten Flächen. In: Höper H, Meesenburg H (eds) *Tagungsband 20 Jahre Bodendauerbeobachtung in Niedersachsen*, GeoBerichte, vol 23. Landesamt für Bergbau, Energie und Geologie, Hannover, pp 163–174
- Koch J, Klose S, Makeschin F (2001) Bioelementverteilung und Humusmorphologie in flugaschebelasteten Oberböden der Dübener Heide. *Berichte Freiburger Forstliche Forschung*, vol 33. Freiburg, pp 183–192
- Lawrence GB, Hazlett PW, Fernandez JJ, Ouimet R, Bailey SW, Shortle WC, Smith KT, Antidormi MR (2015) Declining acidic deposition begins reversal of forest-soil acidification in the northeastern US and eastern Canada. *Environ Sci Technol* 49(22):13103–13111
- Mareschal L, Turpault M-P, Bonnaud P, Ranger J (2013) Relationship between the weathering of clay minerals and the nitrification rate: a rapid tree species effect. *Biogeochemistry* 112(1–3):293–309
- Meesenburg H, Brumme R, Jacobsen C, Meiwes K, Eichhorn J (2009) Soil properties. In: *Functioning and management of European beech ecosystems*. Ecological studies, vol 208. Springer, Berlin, pp 33–47
- Meesenburg H, Ahrends B, Fleck S, Wagner M, Fortmann H, Scheler B, Klinck U, Dammann I, Eichhorn J, Mindrup M (2016) Long-term changes of ecosystem services at Solling, Germany: recovery from acidification, but increasing nitrogen saturation? *Ecol Indic* 65:103–112
- Meiwes K, Meesenburg H, Eichhorn J, Jacobsen C, Khanna P (2009) Changes in C and N contents of soils under beech forests over a period of 35 years. In: *Functioning and management of European beech ecosystems*. Ecological studies, vol 208. Springer, Berlin, pp 49–63

- Möller D, Lux H (1992) Deposition atmosphärischer Spurenstoffe in der ehemaligen DDR bis 1990: Methoden und Ergebnisse. In: Kommission Reinhaltung der Luft im VDI und DIN, vol 18. Düsseldorf, 308 pp.
- Nieder R, Benbi DK, Scherer HW (2011) Fixation and defixation of ammonium in soils: a review. *Biol Fertil Soils* 47(1):1–14
- Piña RG, Cervantes C (1996) Microbial interactions with aluminium. *Biometals* 9(3):311–316
- Reuss JO, Johnson DW (1985) Effect of soil processes on the acidification of water by acid deposition. *J Environ Qual* 14(1):26–31
- Reuss JO, Johnson DW (1986) Acid deposition and the acidification of soils and waters. In: *Ecological studies*, vol 59. Springer, Berlin
- Rich C (1968) Hydroxy interlayers in expansible layer silicates. *Clay Clay Miner* 16(1):15–30
- Riek W, Russ A, Martin J (2012) Soil acidification and nutrient sustainability of forest ecosystems in the northeastern German lowlands – results of the national forest soil inventory. *Folia For Pol Ser A* 54(3):187–195. <https://doi.org/10.5281/zenodo.30835>
- Riek W, Russ A, Kühn D (2015) Waldbodenbericht Brandenburg – Zustand und Entwicklung der brandenburgischen Waldböden. Ergebnisse der landesweiten Bodenzustandserhebungen BZE-2 und BZE-2a. Band 1. Eberswalder Forstliche Schriftenreihe. Landesbetrieb Forst Brandenburg, Landeskompetenzzentrum Forst Eberswalde, Eberswalde
- Schöpp W, Posch M, Mylona S, Johansson M (2003) Long-term development of acid deposition (1880–2030) in sensitive freshwater regions in Europe. *Hydrol Earth Syst Sci* 7(4):436–446
- Schwarz MT, Bischoff S, Blaser S, Boch S, Grassein F, Klarner B, Schmitt B, Solly EF, Ammer C, Michalzik B (2016) Drivers of nitrogen leaching from organic layers in central European beech forests. *Plant Soil* 403(1–2):343–360
- Seip H (1980) Acidification of freshwater-sources and mechanisms. In: *International conference on the ecological impact of acid precipitation*. Sandefjord (Norway). 11–14 Mar 1980
- Spranger T, Lorenz U, Gregor H-D (2015) ICP modelling & mapping: manual on methodologies and criteria for modelling and mapping critical loads & levels and air pollution effects, risks and trends – amended version. UBA Texte, vol 52/2004. Federal Environmental Agency (UBA), Berlin
- Statistik der Kohlenwirtschaft e.V. (2015) <http://www.kohlenstatistik.de/19-0-Braunkohle.html>. Accessed 9 Feb 2015
- Stöcker G, Gluch W (1992) Depositionscharakterisierung auf der Grundlage der Borkenindikation (Biomonitoring). In: Möller D, Lux H (eds) *Deposition atmosphärischer Spurenstoffe in der ehemaligen DDR bis 1990: Methoden und Ergebnisse*. Schriftenreihe der Kommission Reinhaltung Luft im VDI und DIN, vol 18. Düsseldorf, pp 272–287
- Stoddard JL, Jeffries D, Lükewille A, Clair T, Dillon P, Driscoll C, Forsius M, Johannessen M, Kahl J, Kellogg J (1999) Regional trends in aquatic recovery from acidification in North America and Europe. *Nature* 401(6753):575
- Sucker C, von Wilpert K, Puhlmann H (2011) Acidification reversal in low mountain range streams of Germany. *Environ Monit Assess* 174(1–4):65–89. <https://doi.org/10.1007/s10661-010-1758-z>
- Tarrah J, Meiwes KJ, Meesenburg H (2000) Normative calculation of minerals in north German loess soils using the modified CIPW norm. *J Plant Nutr Soil Sci* 163(3):307–312
- Ulrich B (1981) Ökologische Gruppierung von Böden nach ihrem chemischen Bodenzustand. *Z Pflanzenernähr Bodenkd* 144(3):289–305. <https://doi.org/10.1002/jpln.19811440308>
- Ulrich B (1983) Soil acidity and its relations to acid deposition. In: Ulrich B, Pankrath J (eds) *Effects of accumulation of air pollutants in forest ecosystems*. Springer, Dordrecht, pp 127–146
- Ulrich B (1987) Stability, elasticity, and resilience of terrestrial ecosystems with respect to matter balance. In: Schulze E-D, Zwölfer H (eds) *Potentials and limitations of ecosystem analysis*. *Ecological studies*, vol 61. Springer, Berlin, pp 11–49
- Ulrich B (1994) Nutrient and acid-base budget of central European forest ecosystems. In: Godbold DL, Hüttermann A (eds) *Effects of acid rain on forest processes*. Wiley-VCH, New York, NY, pp 1–50

- Ulrich B, Mayer R, Khanna PK (1980) Chemical changes due to acid precipitation in a loess derived soil in Central Europe. *Soil Sci* 130:193–199
- UNECE (1979) Convention on long-range transboundary air pollution (CLRTAP). Geneva
- Waldner P, Marchetto A, Thimonier A, Schmitt M, Rogora M, Granke O, Mues V, Hansen K, Karlsson GP, Zlindra D, Clarke N, Verstraeten A, Lazdins A, Schimming C, Iacoban C, Lindroos AJ, Vanguelova E, Benham S, Meesenburg H, Nicolas M, Kowalska A, Apuhtin V, Napa U, Lachmanova Z, Kristoefel F, Bleeker A, Ingerslev M, Vesterdal L, Molina J, Fischer U, Seidling W, Jonard M, O’Dea P, Johnson J, Fischer R, Lorenz M (2014) Detection of temporal trends in atmospheric deposition of inorganic nitrogen and sulphate to forests in Europe. *Atmos Environ* 95:363–374. <https://doi.org/10.1016/j.atmosenv.2014.06.054>
- Wellbrock N, Bolte A, Flessa H (eds) (2016) Dynamik und räumliche Muster forstlicher Standorte in Deutschland: Ergebnisse der Bodenzustandserhebung im Wald 2006 bis 2008. Thünen Report, vol 43. Johann Heinrich von Thünen Institute, Federal Research Institute for Rural Areas, Forestry and Fisheries, Braunschweig
- Wood SN (2006) Generalized additive models: an introduction with R. Chapman & Hall, Boca Raton, FL
- Wright RF, Larssen T, Camarero L, Cosby BJ, Ferrier RC, Helliwell R, Forsius M, Jenkins A, Kopáček J, Majer V, Moldan F, Posch M, Rogora M, Schöpp W (2005) Recovery of Acidified European Surface Waters. *Environ Sci Technol* 39(3):64A–72A. <https://doi.org/10.1021/es0531778>

Open Access This chapter is licensed under the terms of the Creative Commons Attribution 4.0 International License (<http://creativecommons.org/licenses/by/4.0/>), which permits use, sharing, adaptation, distribution and reproduction in any medium or format, as long as you give appropriate credit to the original author(s) and the source, provide a link to the Creative Commons licence and indicate if changes were made.

The images or other third party material in this chapter are included in the chapter’s Creative Commons licence, unless indicated otherwise in a credit line to the material. If material is not included in the chapter’s Creative Commons licence and your intended use is not permitted by statutory regulation or exceeds the permitted use, you will need to obtain permission directly from the copyright holder.

